Internal Tides and Solitary Waves in the Northern South China Sea: A Nonhydrostatic Numerical Investigation

Ping-Tung Shaw
Dept of MEAS, North Carolina State University
Box 8208, Raleigh, NC 27695-8208
Phone: (919)515-7276 FAX: (919)515-7802 e-mail: pt_shaw@ncsu.edu

Shenn-Yu Chao
Horn Point Laboratory, UMCES
P. O. Box 775, Cambridge, MD 21613-0775
Phone: (410)221-8427 FAX: (410)221-8490 e-mail: chao@hpl.umces.edu

Award Number: N00014-05-1-0280 (NCSU)
Award Number: N00014-05-1-0279 (UMCES)

LONG-TERM GOALS

The goal of this project is to understand processes relevant to the generation, propagation and dissipation of finite-amplitude internal solitary waves observed in the region from the Luzon Strait to the Chinese continental shelf.

OBJECTIVES

With data available from field observations in Non-Linear Internal Wave Initiative (NLIWI), this project is to perform simulation of finite-amplitude internal solitary waves under scenarios in the northern South China Sea. The objective is to provide information on the characteristics of nonlinear internal waves for comparison with data collected from remote sensing, mooring measurements, and shipboard observations.

APPROACH

Processes of wave generation, propagation and dissipation are studied by numerical simulation using a nonhydrostatic ocean model under different scenarios of bottom topography, stratification, and the amplitude of the tidal current. Experiments include wave generation by ridges in the Luzon Strait, wave propagation across the deep basin with an upper-ocean thermocline, wave reflection and diffraction near the Dongsha Island, wave generation and dissipation on the continental slope, and characteristics of higher-mode waves.

WORK COMPLETED

Work is completed in two areas during this year. First, the earlier process study of wave generation and propagation by Shaw et al. (2009) has been quantified using energy fluxes and expanded in the parameter space. The internal wave energy is successfully expressed in terms of nondimensional

Report Documentation Page

Form Approved
OMB No. 0704-0188

1. REPORT DATE	2. REPORT TYPE	3. DATES COVERED
2009		**00-00-2009 to 00-00-2009**

4. TITLE AND SUBTITLE	5a. CONTRACT NUMBER
Internal Tides and Solitary Waves in the Northern South China Sea: A Nonhydrostatic Numerical Investigation	5b. GRANT NUMBER
	5c. PROGRAM ELEMENT NUMBER
6. AUTHOR(S)	5d. PROJECT NUMBER
	5e. TASK NUMBER
	5f. WORK UNIT NUMBER
7. PERFORMING ORGANIZATION NAME(S) AND ADDRESS(ES) **North Carolina State University,Dept of MEAS,Box 8208,Raleigh,NC,27695-8208**	8. PERFORMING ORGANIZATION REPORT NUMBER
9. SPONSORING/MONITORING AGENCY NAME(S) AND ADDRESS(ES)	10. SPONSOR/MONITOR'S ACRONYM(S)
	11. SPONSOR/MONITOR'S REPORT NUMBER(S)

12. DISTRIBUTION/AVAILABILITY STATEMENT
Approved for public release; distribution unlimited

13. SUPPLEMENTARY NOTES

14. ABSTRACT

15. SUBJECT TERMS

16. SECURITY CLASSIFICATION OF:			17. LIMITATION OF ABSTRACT	18. NUMBER OF PAGES	19a. NAME OF RESPONSIBLE PERSON
a. REPORT **unclassified**	b. ABSTRACT **unclassified**	c. THIS PAGE **unclassified**	**Same as Report (SAR)**	**7**	

parameters. The parametric dependence will be verified in a graduate student's Ph. D. thesis research. In another study, satellite and mooring data collected during 2005 have been used to study the variation in the wave propagation speed from Luzon Strait to the continental margin of the northern South China Sea. A master thesis is produced (Kim, 2009).

RESULTS

Generation of internal solitary waves in the northern South China Sea is demonstrated as a two-step process by Shaw et al. (2009). Internal waves are generated by the barotropic tidal flow over a steep ridge in the form of slanting wave beams, as demonstrated in the classical laboratory experiment of Mowbray and Rarity (see Gill, 1982, p. 137). When reaching a shallow thermocline, the internal wave beams are trapped in a wave guide, producing horizontally-propagating internal tides. If the wave amplitude is large, the internal tide intensifies to form internal solitary waves. From the weakly nonlinear theory, one important parameter governing the formation of wave beams is the ratio of the ridge slope to that of the wave beam. Internal waves are produced when the slope of the ridge is steeper than that of the internal wave beam. Using a nonhydrostatic model, Shaw et al. (2009) verified that this parameter is critical in the generation of internal solitary waves over a finite ridge in an ocean with a depth-varying buoyancy frequency profile similar to that in the Luzon Strait.

A quantitative description of the dependence of internal wave energy on the ridge slope and stratification is obtained this year. As in the study of Shaw et al. (2009), the model of Shaw and Chao (2006) is used. The simulation adopts a density profile similar to that in the upper ocean of the northern South China Sea. The buoyancy frequency is given by $N = N_0 \cosh^{-1}\left(\frac{z - z_0}{D}\right)$, where N_0 = 0.015 rad/s, z_0 = –50 m, and D = 120 m. The value of the buoyancy frequency is large in the upper 200 m of the water column and decreases rapidly with increasing depth. Forcing is at the semidiurnal tidal period. A bell-shaped ridge is used with bottom depth at $z = -H + \frac{h_0}{1 + (x/L)^2}$, where H = 800 m is the bottom depth away from the ridge, h_0 = 400 m, and L is the half-width of the ridge.

An interesting result obtained from the simulation is the contrast in internal wave energy over ridges of different widths. Figure 1 shows the total internal wave energy generated over a ridge of half-width L = 15 km at 2, 4 and 6 hours after the slack tide. The tidal current is toward right in the top two panels and zero in the bottom panel. Energy propagates away from the ridge in wave beams following the development of the barotropic tidal current. Shaw et al. (2009) demonstrated that strong internal wave beams are generated over the ridge and evolve into internal solitary waves when this ridge is placed 200 m below the surface in waters of strong stratification. In Figure 1, the ridge top is below the thermocline in waters of much weaker stratification. Nevertheless, the process of internal wave generation is qualitatively similar except that the energy is reduced to about 1/3 of the previous value. In contrast, the pattern of wave energy over a ridge of half width L = 60 km is qualitatively different (Figure 2). Wave energy shows a normal-mode structure over the ridge. The internal wave in this case is much weaker. Energy converted to the internal wave is about 10 times less than in Figure 1.

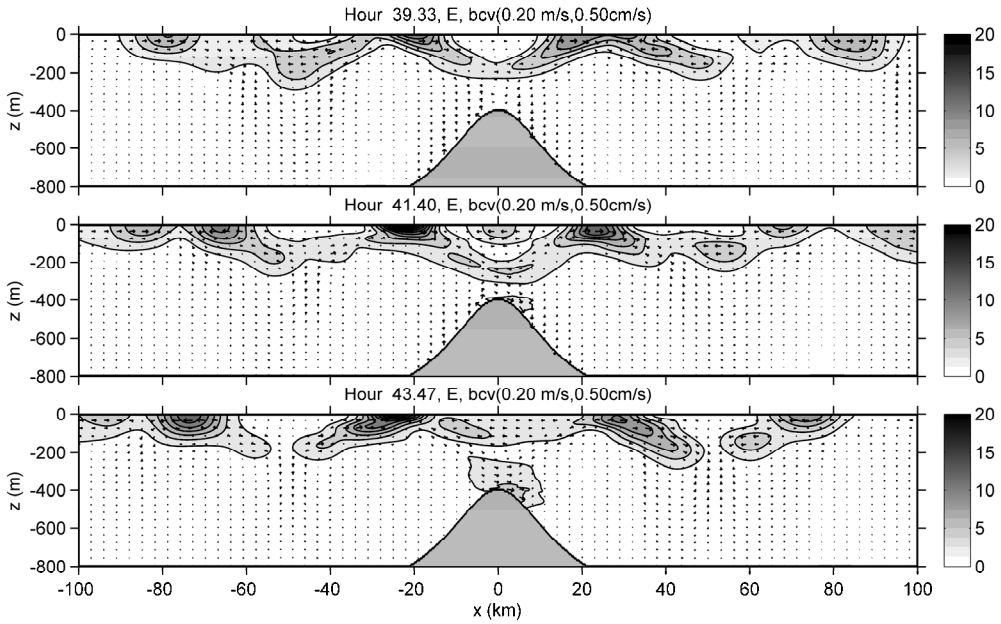

Figure 1. Energy of internal waves in J/m^3 at a ridge of half width L = 15 km at 2, 4 and 6 hours after the slack water. Tidal current is toward right. The contour interval is 2 J/m^3. Vectors show the baroclinic velocity. A vector of size of the grid box is 0.2 m/s and 0.5 cm/s in the horizontal and vertical directions, respectively.

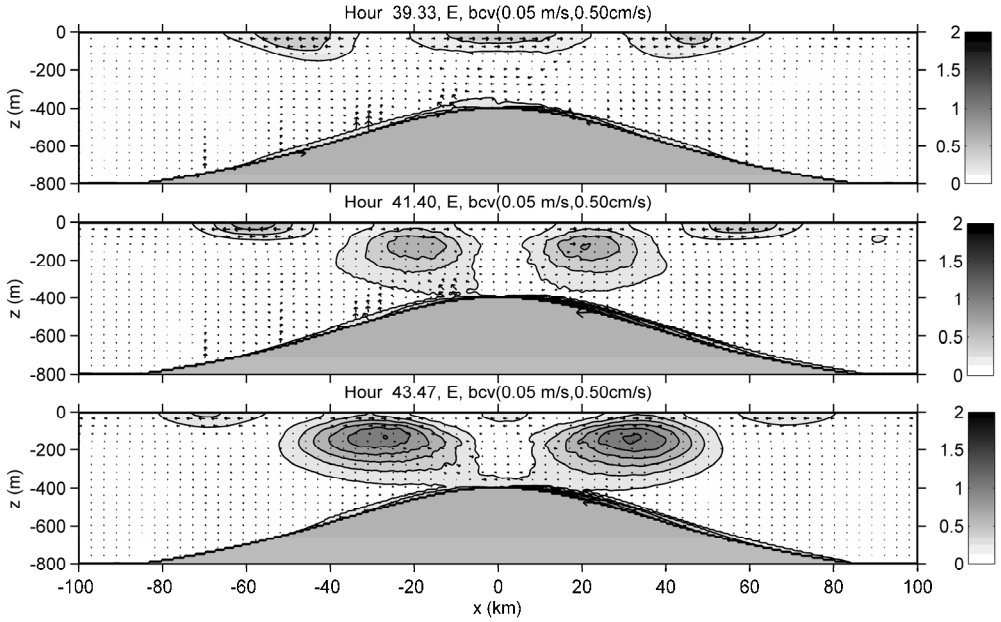

Figure 2. Same as Figure 1 but for ridge half- width L = 60 km. The contour interval is 0.2 J/m^3. A vector of size of the grid box is 0.05 m/s and 0.5 cm/s in the horizontal and vertical directions, respectively.

The wave patterns corresponding to these two scenarios are demonstrated in the perturbation density field in Figure 3. In the upper panel, wave beams form over a steep ridge and develop into first-mode waves at 80 km away from the origin. Over a ridge of gentle slope in the lower panel, waves of first vertical mode develop over the ridge and evolve into mode-one waves. The phase of the wave outside the influence of ridge topography is similar in both cases except that the wave amplitude is much reduced over a ridge of gentle slope.

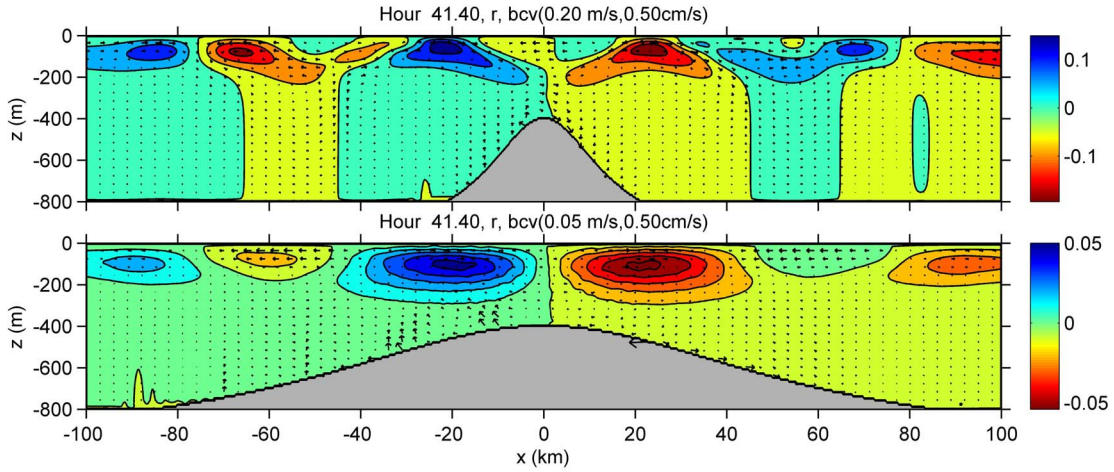

Figure 3. Perturbation density in kg/m^3 at 4 hours after the slack water for ridges of half width L = 15 km (top panel) and L = 60 km (bottom panel). The contour interval is 0.05 and 0.01 kg/m^3 in the top and bottom panels, respectively. Vectors show the baroclinic velocity with the scales for (u,v) in parentheses.

The vertical energy flux associated with the energy field in Figures 1 and 2 is shown in Figures 4 and 5, respectively. Energy propagates upward from a narrow band over a ridge of steep slope (Figure 4). The path is more vertical in deep water and slants toward horizontal in the strongly stratified water above 200 m. The wave beam is reflected downward by the surface. Since the ridge is narrow, downward flux reaches the deep water beyond ridge topography, the region of strong upward energy flux. This process traps the wave beam in the upper-ocean wave guide, resulting in mode-one internal waves propagating away from the ridge. In the case of a gentle ridge slope (Figure 5), upward energy flux is over a wide horizontal distance, preventing the development of wave beams. Upward energy flux dominates below 200 m depth over the ridge, while surface reflection appears as a region of broad downward energy flux above 200 m. The mechanisms of wave generation are quite different in these two cases. Although similar internal tides appear beyond a ridge, development of wave beams is essential in producing strong internal tides.

IMPACT/APPLICATIONS

The ratio of the topographic slope to the slope of the wave beam has been used as an important parameter for internal wave generation in an ocean with constant buoyancy frequency (e.g., Garrett and Kunze (2007). It is not clear how the ratio should be defined in an ocean with depth-varying stratification. In Figure 1, the slope of the wave beam calculated from the buoyancy frequency at the depth of the ridge is much greater than the slope of the ridge. Thus it is inappropriate to use the local buoyancy frequency at the ridge depth to calculate the slope of the wave beam. The present study

shows that the horizontal distance traveled by a wave beam from the ridge top to the sea surface relative to the ridge width is a better measure of the effectiveness in energy conversion from the barotropic tide to internal waves. A nondimensional equation has been developed to estimate the energy conversion rate using the ratio of the maximum topographic slope to the mean slope of the wave beam in the water column above the ridge. This relation is being tested over a wide range of parameters using the data from the nonhydrostatic simulation.

RELATED PROJECTS

We have collaborated with Dong Shan Ko to develop oceanic applications from the ideas obtained from numerical study. Data from real-time simulation at NRL (Ko et al., 2008) are being used to predict the energy flux using stratification, topography and the strength of the tidal current. Dr. Ko is also working on transition of internal wave prediction capabilities to operational use; P.-T. Shaw serves as a member of the panel for validation and test of that study.

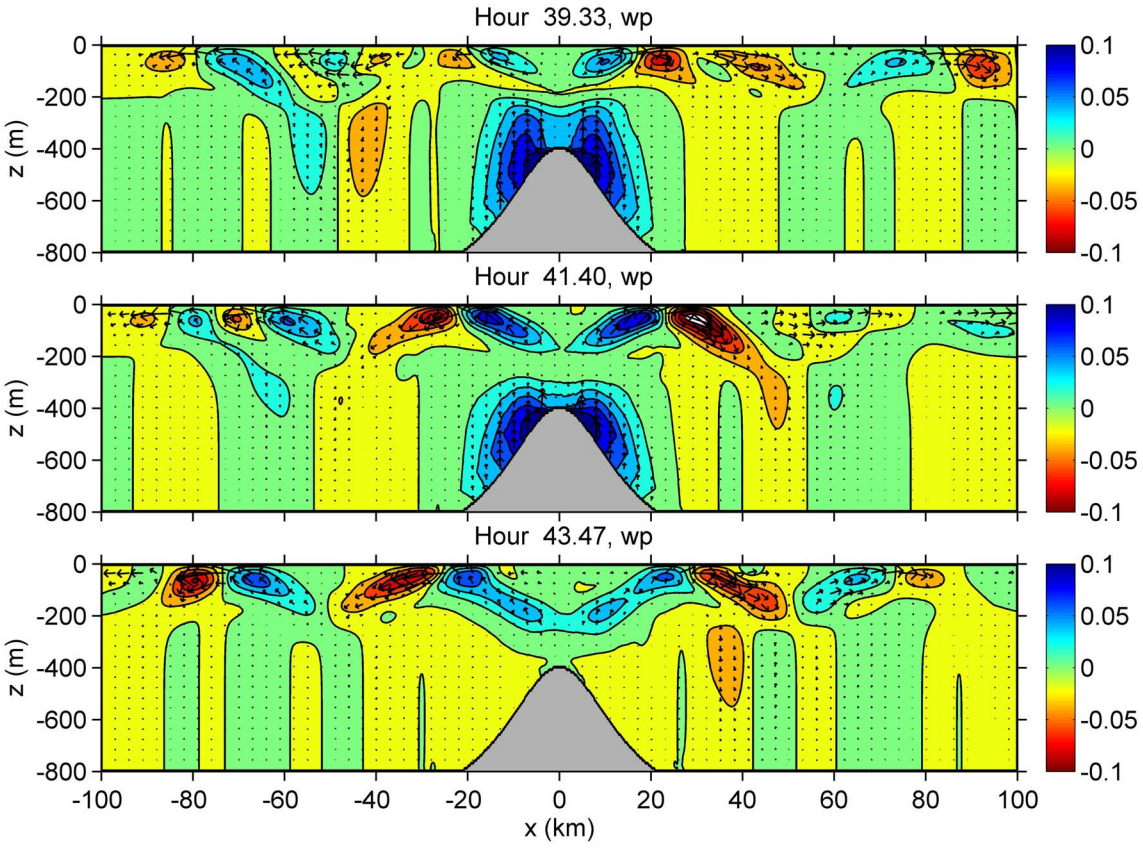

Figure 4. Internal wave beams in the plots of the vertical energy flux (W/m) for a ridge of half width L = 15 km. The contour interval is 0.02 W/m. Vectors show energy flux; a vector between two consecutive grid points represents 10 and 0.1 W/m in the horizontal and vertical directions, respectively.

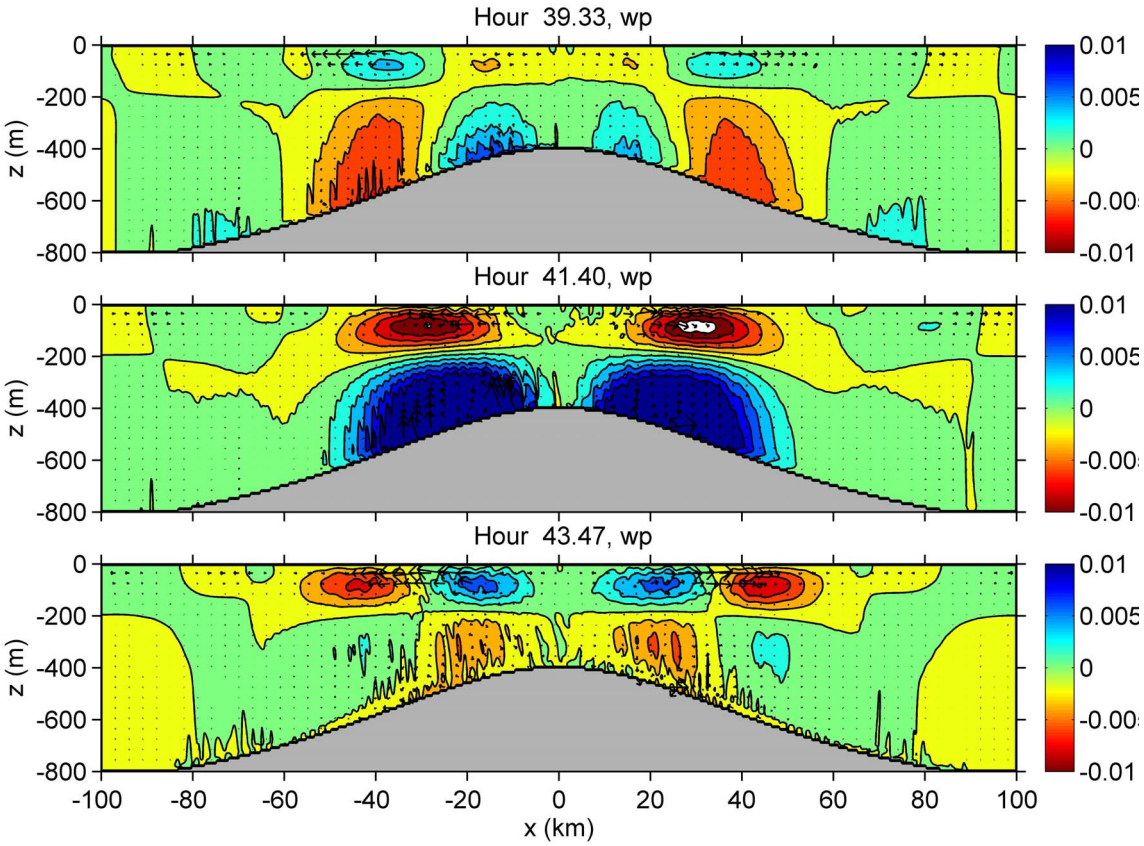

Figure 5. No internal wave beam develops in the plots of the vertical component of energy flux (W/m) for a ridge of half width L = 60 km. The contour interval is 0.002 W/m. Vectors show energy flux; a vector between two consecutive grid points represents 1 and 0.05 W/m in the horizontal and vertical directions, respectively.

REFERENCES

Gill, A. E. (1982) Atmosphere-Ocean Dynamics, Academic Press, New York.

Garrett, C. and E. Kunze (2007) Internal tide generation in the deep ocean, Annu. Rev. Fluid Mech., 39, 57–87.

Kim, S.-P., (2009) Internal tides and internal solitary waves in the northern South China Sea. Master of Science thesis, Dept. Marine, Earth and Atmospheric Sciences, North Carolina State Univ.

Ko, D.S., P.J. Martin, C.D. Rowley, and R.H. Preller, (2008) A Real-Time Coastal Ocean Prediction Experiment for MREA04. J. Marine Systems 69, 17-28. doi:10.1016/j.jmarsys.2007.02.022.

Shaw, P.-T., and S.-Y. Chao (2006) A nonhydrostatic primitive-equation model for studying small-scale processes: an object oriented approach, Continental Shelf Res., 26, 1416-1432.

Shaw, P.-T., D. Ko, and S.-Y. Chao (2009) Internal solitary waves induced by flow over a ridge: with applications to the northern South China Sea, J. Geophys. Res., 114, C02019, doi:10.1029/2008JC005007, 2009.

PUBLICATIONS

P.-T. Shaw, D.-S. Ko and S.-Y. Chao (2009) Internal solitary waves induced by flow over a ridge: with applications to the northern South China Sea, Journal of Geophysical Research, 114, C02019, doi:10.1029/2008JC005007, 2009. [published, refereed]

Ko, D. S., S.-Y. Chao, P. Huang, and S. F. Lin (2009) Anomalous upwelling in Nan Wan: July 2008, Terrestrial, Atmospheric and Oceanic Sciences, [in press, refereed]